Building and Environment 138 (2018) 124–134

Contents lists available at ScienceDirect

Building and Environment

journal homepage: www.elsevier.com/locate/buildenv

# Pilot study of the vertical variations in outdoor pollutant concentrations and environmental conditions along the height of a tall building

Parham Azimi[a], Haoran Zhao[a], Torkan Fazli[a], Dan Zhao[a], Afshin Faramarzi[a], Luke Leung[b], Brent Stephens[a,*]

[a] Department of Civil, Architectural, and Environmental Engineering, Illinois Institute of Technology, Chicago, IL, USA
[b] Skidmore, Owings & Merrill LLP, Chicago, IL, USA

ARTICLE INFO

*Keywords:*
Indoor air quality
Tall buildings
Ventilation
Particulate matter
Ozone
Urban environment

ABSTRACT

It is generally assumed that vertical pollutant dispersion can reduce exposures to ambient pollutants in tall buildings, as concentrations of some ground-source pollutants are diluted at higher floors. However, we are aware of very few measurements of airborne pollutant concentrations that have been made specifically along the height of tall buildings. Therefore, we conducted a pilot study to measure the vertical variation in the concentrations of several outdoor pollutants and environmental parameters along the height of a ~60-story (~300 m) building in downtown Chicago, IL during a one-week period in the summer of 2017. Simultaneous measurements of concentrations of size-resolved particulate matter 0.3–10 μm (which were also used to estimate $PM_1$, $PM_{2.5}$, and $PM_{10}$ mass concentrations), ozone ($O_3$), nitrogen dioxide ($NO_2$), carbon dioxide ($CO_2$), and carbon monoxide (CO), as well as temperature and relative humidity, were made using multiple sets of instrumentation installed in the outdoor air intakes of the mechanical systems upstream of any filtration or mixing processes on the 2nd, 16th, 29th, and 44th floors and in an open-air area on the 61st floor. The average $PM_1$ and $PM_{2.5}$ concentrations estimated on the top two floors were more than 30% lower than on the 2nd floor. Temperature, humidity ratio, and $CO_2$ concentrations decreased with height, $O_3$ concentrations increased with height, and $NO_2$ concentrations were less consistent. Most of the differences between floors were statistically significant. Floor height was more strongly correlated with $PM_1$, $PM_{2.5}$, $PM_{10}$, $CO_2$, and $O_3$ concentrations than with local wind speed and direction.

## 1. Introduction

Elevated outdoor concentrations of airborne pollutants such as particulate matter, ozone, and oxides of nitrogen have been consistently associated with increased risks of respiratory symptoms, mortality, and lung cancer [1–7]. Concentrations of many of these pollutants have increased in many urban environments globally in recent years [8–10]. Associations between outdoor pollutant concentrations and adverse health effects are typically made in large epidemiological studies using stationary ambient measurements with inlet heights of ~2–~15 m [11]. However, because outdoor pollutants can infiltrate and persist indoors where Americans spend the majority of their time [12], much of their exposure to pollutants of outdoor origin often occurs inside buildings [13–20]. Indoor exposures to outdoor pollutants are a function of several key factors including outdoor air ventilation rates, envelope pollutant penetration efficiency, HVAC filtration efficiency, indoor pollutant deposition rates, and, importantly, outdoor pollutant concentrations at the source of ventilation air [21]. While previous research has assessed many of these parameters in smaller residential and commercial buildings [22,23], very few measurements have ever been made in tall buildings where inlet heights for outdoor air can be hundreds of meters above ground level.

Most previous studies on vertical pollutant dispersion or the vertical distribution of other environmental parameters in urban street canyons have relied on computational fluid dynamics (CFD) simulations [24–26] or wind tunnel experiments [27–29]. There have been very few field measurements of the vertical dispersion of outdoor pollutants specifically along the height of tall buildings. As an example, one recent study of a mid-rise (i.e., ~22 stories, or ~55 m tall) building in Chile showed that outdoor ozone concentrations were found to increase with height [30]. Measured outdoor ozone concentrations were approximately 10–15% higher on the 21st story (53 m above ground level) than on the 3rd story (6 m above ground level). These measurements suggest that occupants of the higher floors in this building may be exposed to

* Corresponding author. Department of Civil, Architectural and Environmental Engineering, Illinois Institute of Technology, 3201 S Dearborn Street, Alumni Hall Room 228, Chicago, IL 60616, USA.
*E-mail address:* brent@iit.edu (B. Stephens).

https://doi.org/10.1016/j.buildenv.2018.04.031
Received 29 January 2018; Received in revised form 23 April 2018; Accepted 24 April 2018
Available online 26 April 2018
0360-1323/ 

higher indoor concentrations of outdoor ozone, depending on detailed ventilation system characteristics such as ventilation rates and the location of the outdoor air intakes.

Other limited previous experimental research, while not necessarily sampling in and around tall buildings, has shown that outdoor pollutant concentrations can vary greatly with elevation within the range of height of many tall buildings [31]. Perhaps most relevant to tall (i.e., < 300 m) and super-tall (i.e., > 300 m) buildings [32], aircraft measurements have shown that the vertical variation in outdoor ozone concentrations may be even greater at higher elevations. For example, one study showed that the highest outdoor ozone concentrations during nighttime periods were observed above 200 m (note that 200 m roughly corresponds to ~55 stories with typical floor height) [33]. This variation was more scattered during mornings and afternoons, but still suggested an overall similar pattern. These data suggest that occupants on the highest floors of tall or super-tall buildings may be subjected to more than twice the outdoor ozone concentrations than someone in the bottom third floors of the same building, depending on a number of detailed HVAC system characteristics. Vertical variations in outdoor ozone concentrations tend to vary with the height of the atmospheric boundary layer [34], which can vary highly between rural and urban environments and can vary diurnally [35,36]. There is also strong experimental evidence from ambient monitoring that outdoor particulate matter concentrations often decrease with building height [37,38], potentially offering a protective effect at higher floors. However, very few measurements of the vertical variation in outdoor pollutant concentrations exist, particularly along the height of tall buildings in urban environments.

Despite the lack of measurements to date, a study in Switzerland recently suggested that differences in environmental exposures may have contributed to reductions in all-cause mortality that were associated with increasing residential floor height in buildings [39]. Similarly, a study of office buildings in the U.S. found significantly higher building-related symptoms reported by occupants working on the floors of buildings that had outdoor air intakes less than 60 m above ground level, which may have been due to greater levels of pollutants from vehicles at air intakes nearer the ground level [40]. The need to better understand pollutant exposures in tall buildings is growing, as there are now a total of over 1300 buildings taller than 200 m in the world, with 144 (11% of the total) being completed in 2017 alone [41]. To begin to fill this knowledge gap, here we report results from a pilot study in which we measured the vertical variation of several outdoor pollutants and environmental parameters along the height of a single tall building in downtown Chicago, IL, USA. The aim is to quantify the dispersion of ambient pollutant concentrations and environmental parameters measured along the height of the test building and to determine the importance of building height and local meteorological factors in influencing the observed variability in the resulting data.

## 2. Material and methods

A single tall building in Chicago, IL, USA, was recruited for measurements. The building, which will remain unnamed and whose ownership will not be identified, was approximately 60 stories (~300 m) tall. Time-resolved measurements were conducted over one weeklong period from June 22, 2017 to June 29, 2017 to monitor concentrations of size-resolved particulate matter (PM), ozone ($O_3$), nitrogen dioxide ($NO_2$), carbon dioxide ($CO_2$), carbon monoxide (CO), and temperature and relative humidity along the height of the tall building. To best represent outdoor air coming into the building, simultaneous measurements were made using multiple sets of instruments placed in the outdoor air intakes on the mechanical systems located on four different floors (i.e., the 2nd, 16th, 29th, and 44th floors), as well as in an open-air area on the 61st floor located underneath a ~2 m high metal rack on which a cooling tower was located. The location of measurements within the outdoor air intakes was upstream of any filtration or mixing processes. Measurements were made within approximately 0.2 m downstream of a coarse metallic grate located on the exterior facade of the building through which outdoor air flowed, and approximately 3 m upstream from adjustable louvers that were located downstream of the exterior grate. The louvers controlled mixing between outdoor air and return air, and were located 2–3 m upstream of a downstream filter bank. A photo of the measurement location in one outdoor air intake is shown in the SI (Fig. S1).

### 2.1. Instrumentation

The following sections describe the instruments that were used to measure pollutant concentrations and environmental conditions in the five sampling locations along the vertical height of the test building.

#### 2.1.1. Particulate matter (PM)

MetOne GT-526S optical particle counters (OPCs) were used to measure size-resolved optical particle concentrations for particles from 0.3 to 10+ μm in optical diameter in 6 size bins: 0.3–0.5 μm, 0.5–1 μm, 1–2 μm, 2–5 μm, 5–10 μm, and 10+ μm [42]. We primarily used estimates of PM mass concentrations rather than number concentrations for the analyses herein because of their greater, or at least better known, implications for human health. However, we also show the measured size-resolved particle number concentrations in the results section and in the SI.

To estimate integral PM mass concentrations, the mass concentration of particles in each size bin smaller than 10 μm was estimated by assuming spherical particles with diameter equal to the geometric mean diameter of each size bin and uniform density of 1.5 g/cm$^3$ for all particle sizes [43,44]. The mass concentration of $PM_1$, $PM_{2.5}$, and $PM_{10}$ was then estimated by adding the mass of particles in the size bins associated with each fraction, as shown in Equations (1)–(3) [45–47]. The assumption for uniform particle density is taken from existing literature sources and may not be accurate for the Chicago area [48–50]. Further, this approach does not account for any mass below 0.3 μm, which will greatly underestimate total number concentrations and may also underestimate PM mass concentrations [51]. However, for the purposes of this study (i.e., to explore the pattern of pollutant concentrations measured along the height of the test building), only repeatable, not absolutely accurate, PM measurements are required on each floor.

$$C_{PM1} = \left(\frac{1}{6}\pi d_{0.3-0.5}^3 \rho N_{0.3-0.5} + \frac{1}{6}\pi d_{0.5-1.0}^3 \rho N_{0.5-1.0}\right) \times 10^{-6} \quad (1)$$

$$C_{PM2.5} = \left(\frac{1}{6}\pi d_{0.3-0.5}^3 \rho N_{0.3-0.5} + \frac{1}{6}\pi d_{0.5-1.0}^3 \rho N_{0.5-1.0} + \frac{1}{6}\pi d_{1.0-2.0}^3 \rho N_{1.0-2.0} + \frac{1}{6}\pi d_{2.0-2.5}^3 \rho N_{2.0-5.0} \times \frac{\log 2.5 - \log 2.0}{\log 5.0 - \log 2.0}\right) \times 10^{-6} \quad (2)$$

$$C_{PM10} = \left(\frac{1}{6}\pi d_{0.3-0.5}^3 \rho N_{0.3-0.5} + \frac{1}{6}\pi d_{0.5-1.0}^3 \rho N_{0.5-1.0} + \frac{1}{6}\pi d_{1.0-2.0}^3 \rho N_{1.0-2.0} + \frac{1}{6}\pi d_{2.0-5.0}^3 \rho N_{2.0-5.0} + \frac{1}{6}\pi d_{5.0-10}^3 \rho N_{5.0-10}\right) \times 10^{-6} \quad (3)$$

where $C_{PM1}$, $C_{PM2.5}$, and $C_{PM10}$ are the mass concentrations of $PM_1$, $PM_{2.5}$, $PM_{10}$, respectively (μg/m$^3$); $d_{i\text{-}j}$ is the geometric mean of particle diameter sizes from $i$ to j (μm); ρ is the assumed particle density (1.5 g/cm$^3$); and $N_i$ is the particle number concentration measured in size range $i$ (#/m$^3$). To estimate $PM_{2.5}$ mass concentrations, we used a log-basis differential method to estimate the mass concentration in the 2–2.5 μm size range based on measurements in the 2–5 μm size bin. The number concentration in a virtual size bin of 2–2.5 μm was estimated by multiplying the number concentration of the default 2–5 μm size bin by the ratio of the logarithmic difference of the virtual 2–2.5 μm and actual 2–5 μm size bins (i.e., (log2.5 − log2)/(log5 − log2)).

#### 2.1.2. Gaseous pollutants: $O_3$, $NO_2$, $CO_2$, and CO

Aeroqual SM50 OEM gas-sensitive semiconductor (GSS) ozone monitors (0–0.5 ppm) were used to measure ozone concentrations with a manufacturer-reported accuracy of ± 15% and a lower limit of detection (LOD) of 1 ppb. These monitors have recently be shown to have accuracy comparable to research and regulatory grade equipment [52], particularly at ambient concentrations well above the reported LOD. Aeroqual S500 monitors with gas-sensitive electrochemical (GSE) $NO_2$ sensor heads were used to measure $NO_2$ concentrations with a manufacturer-reported accuracy of ± 20 ppb, a resolution of 1 ppb, and a limit of detection of 5 ppb. These instruments have been used successfully in a few recent studies of indoor and outdoor microenvironments of which we are aware [53–55], and have been shown to be reasonably accurate after calibration with higher-grade equipment.

Lascar EL-USB-CO300 CO monitors were used to measure CO with a manufacturer-reported accuracy of ± 6% of reading and a resolution of 0.5 ppm. These inexpensive instruments are typically most useful when there are large CO sources from combustion (e.g., environmental tobacco smoke or water pipe smoking) [56,57], but other recent residential indoor investigations have used them with success as well [58]. Extech SD800 dual wavelength non-dispersive infrared (NDIR) $CO_2$ monitors were used to measure $CO_2$ concentrations with an accuracy of ± 40 ppm for concentrations less than 1000 ppm or ± 5% of the reading for concentrations greater than 1000 pm. They have been used in prior successful demonstrations by other field research teams [58]. However, we do not report any of the data from the CO data loggers because the outdoor CO concentration was consistently below the LOD of the CO monitors; thus, the monitors recorded zero values for the vast majority of the measurement intervals.

#### 2.1.3. Environmental conditions

Onset HOBO U12-013 2-Channel Temperature/Relative Humidity (RH) data loggers were used for logging data from the Aeroqual SM50 OEM ozone monitors as well as measuring the temperature and relative humidity of the ambient air. The humidity ratio at each recorded interval was calculated based on the temperature and relative humidity readings following procedures described in the ASHRAE Handbook of Fundamentals [59]. Moreover, we obtained data for wind speed and wind direction from the same time period as the field measurements from a nearby weather station via the Weather Underground Personal Weather Station Network [60]. These data were reported typically at 5-min intervals (albeit with some variation throughout the week), and were summarized as hourly averages for subsequent analyses.

#### 2.1.4. Instrument calibrations

Because multiple versions of each instrument were used to measure each parameter on each of the five floors simultaneously, instrument calibration was conducted using a combination of approaches either before or after the field measurements occurred. At least one of two types of calibrations was performed for each instrument: (1) co-locations against factory-calibrated research-grade instruments and/or (2) co-locations against other instruments of the same type, assuming one serves as an arbitrary reference. The former approach allows raw data from each instrument to be adjusted to provide a reasonably accurate measure of the absolute value of the parameter in question. The latter approach allows raw data from each instrument to be adjusted to provide a reasonably accurate measure of the relative value of the parameter compared to an arbitrary reference instrument. Calibration procedures and resulting data are reported in full for each instrument in the SI.

A summary of the calibration results is as follows. The Onset temperature and relative humidity loggers and the Lascar CO loggers were not calibrated based on past experience demonstrating little need to do so. The Aeroqual SM50 $O_3$ monitors were successfully calibrated using a research grade instrument (2B Technologies Model 211) as a reference, although the instruments were shown to have a fairly high limit of detection (LOD). The highest observable LOD was ~30 ppb; thus, all data below 30 ppb were excluded from analysis to allow for a fair comparison between instruments on each floor. The MetOne OPCs, Extech $CO_2$ monitors, and the Aeroqual S500 $NO_2$ monitors were successfully calibrated using one of the same instruments as an arbitrary reference. The arbitrary reference in all cases was chosen to be the instrument that was deployed on the lowest floor (i.e., the 2nd floor) in the field-testing.

### 2.2. Field measurement methods

All five sets of instruments described in Section 2.1 were placed in the top drawer in five identical rolling tool carts with uninterruptible power supplies installed in the bottom drawer. The top drawer of each rolling tool cart was modified to include a small exhaust fan on one side and 12 small holes for air intake drilled on the opposite side to continuously draw in sample air flow (Fig. S1). A team of researchers distributed the monitoring instruments to be installed on the 2nd, 16th, 29th, 44th, and 61st floors with the help of the building's facilities and engineering personnel. In the mechanical rooms, the rolling tool carts were placed as close as possible to the exterior grates on the outdoor air intakes and a box fan was operated continuously to ensure that outdoor air was flowing into the plenum area even if/when the HVAC outdoor air intake happened to shut off for periods of time. Unfortunately we do not have data on the operation of the outdoor air dampers or the operation of HVAC systems. For the 61st floor installation, the rolling tool cart was placed underneath a cooling tower stand that was approximately 2 m tall and located in an otherwise open area that provided for substantial outdoor air flow to the instrument cart.

All of the instruments were synchronized to collect data at approximately the same time. First, we set the internal clock of all instruments to be consistent immediately before the field deployment. The Onset HOBO data loggers recorded the outdoor temperature and relative humidity and data from the SM50 ozone monitors at 1-min intervals using the setting “at interval” to synchronize. Therefore, no additional synchronization was needed for those measurements. The same was true for the CO data loggers, which synchronized with the CPU clock that was used to launch the devices. In order to launch the other monitors simultaneously, individual researchers were deployed to each floor and communicated via two-way radios to manually initiate data logging on each instrument at the same interval at approximately the same time. The result is a set of data that includes synchronized time-stamped data for which each instrument for each measurement type is synchronized to the other instruments with the same measurement type, while all measurement types are synchronized to within approximately 30 s of each other (or closer).

The monitors were then left to record data for approximately one week. The SM50 ozone monitors, the SD800 $CO_2$ monitors, and the HOBO T/RH data loggers successfully collected data for the entire period while synchronized at 1-min intervals, while the GT-526S OPCs successfully collected data for one week at 2-min intervals (there was not enough storage space on the OPCs to collect data for the entire week at 1-min intervals). The S500 $NO_2$ monitors recorded data at 1-min intervals for only the last ~5.5 days of the weeklong measurements because their internal memory cards were filled and the earlier data points were automatically overwritten.

### 2.3. Data analysis

Upon data collection, calibration factors were applied to the raw data collected from each instrument following procedures described in the SI. Reported measurements are not corrected for air temperature or density, as volume corrections for air density are estimated to be less than 3% at maximum along the ~300 m height of the test building. We explored the resulting data set in the following ways: (1) time-series plots; (2) box plots and summary statistics for each floor and building

height; (3) diurnal patterns in differences across floors; (4) statistical significance testing of simultaneous measurements between floors; and (5) statistical significance testing of measurements compared to floor height and records of wind speeds and directions from a nearby weather station.

To evaluate the statistical significance of the floor-by-floor comparisons, we conducted nonparametric Wilcoxon signed-rank tests to make paired comparisons of each simultaneously measured parameter (e.g., temperature, humidity ratio, $PM_1$, $PM_{2.5}$, $PM_{10}$, $O_3$, $NO_2$, and $CO_2$, measured at either 1- or 2-min intervals) across the five floors. We used p-values adjusted for the sample size to determine statistical significance (i.e., $p = 1–(1–0.05)^{1/n}$, where n = the number of recorded data points for each instrument). To evaluate the statistical significance of comparisons between parameter measurements and floor height, wind speeds, and wind directions, we calculated nonparametric Spearman rank correlation coefficients between hourly averages of each value using Stata Version 12 (StataCorp, College Station, TX).

## 3. Results and discussion

In each subsection below, floor-by-floor comparisons of synchronized parameter measurements are shown using box plots that show the interquartile range (IQR) as the 25th and 75th percentile values (boxes), median values (line within the boxes), the upper and lower adjacent values (i.e., the upper or lower quartile plus/minus 1.5 times the IQR), and any outside values as dots (unless excluded for clarity) (i.e., Figs. 1–4). Time-series data from the same measurements are also shown in the SI, and average ( ± standard deviation) values for all parameters are plotted versus approximate building height in Fig. 5. Table S1 provides a full statistical summary of the calibrated results and also calculates the relative difference in the arithmetic means of each measured parameter from each floor compared to the 2nd floor as the closest-to-ground-level reference. Results from statistical significance testing of simultaneous measurements on each floor are shown in Table 1.

### 3.1. Temperature and humidity ratio

Fig. 1 shows box plots of the temperature and humidity ratio data measured on the five floors. Full weeklong time-series data are shown in Figs. S18 and S19. Humidity ratio is shown instead of relative humidity because it is an absolute measure of humidity and it is not a function of temperature. The average temperature across all floors ranged from ~21.5°C to ~24.0°C throughout the week, with minimum and maximum values ranging from ~14°C to ~32°C. The average temperature was ~2.8% higher on the 16th floor compared to the 2nd floor, but was ~1.7% (i.e., ~0.4°C), ~2.3% (i.e., ~0.5°C), and ~7.6% (i.e., ~1.7°C) lower on the 29th, 44th, and 61st floors compared to the 2nd floor, respectively. All measured temperature differences between floors were statistically significant (Table 1).

The average temperature difference of ~1.7 °C between the 61st floor (height of ~300 m) and the 2nd floor (height of ~5 m) yields an average temperature lapse rate of about −0.58 °C per 100 m along the height of the building, which is within ~10% of the commonly used Standard Lapse Rate of −6.5 °C per 1000 m (i.e., −0.65 °C per 100 m) [61,62]. However, the temperature lapse was not constant across each floor comparison, which suggests that the temperature lapse rate assumption for a building of this size in this urban context may not be linear and may be influenced by other factors such as surrounding buildings or highly localized meteorological conditions [63].

The average relative humidity across all floors ranged from ~45% to ~51% throughout the week, with minimum and maximum values ranging from ~26% to ~77%. The average relative humidity was ~9.1%, ~5.5%, and ~4.8% lower on the 16th, 29th, and 44th floors compared to the 2nd floor, respectively, but was ~4.8% higher on the 61st floor compared to the 2nd floor. Differences in RH were not as consistent as differences in humidity ratio because of the dependence of RH on temperature. The average humidity ratio across all floors was ~0.0084 $kg_w/kd_{ga}$ throughout the week, with minimum and maximum values ranging from ~0.005 $kg_w/kd_{ga}$ to ~0.016 $kg_w/kd_{ga}$. The average absolute humidity ratio was ~5.2%, ~7.9%, ~8.0%, and ~5.1% lower on the 16th, 29th, 44th, and 61st floors compared to the 2nd floor, respectively. There was no clear linear trend observed between humidity ratio and building height, but humidity ratio was lower on all floors above ground level. All differences in relative and absolute humidity measured between floors were statistically significant except the comparison of humidity ratio between the 16th and 61st floors (Table 1).

### 3.2. Particulate matter (PM)

#### 3.2.1. Size-resolved particle number concentrations

Fig. 2 shows box plots of size-resolved particle number concentrations measured on each floor. Outside values (i.e., those above/below the upper/lower adjacent values) are not shown for visual clarity. Fig. S20 shows full weeklong time-series particle number concentration data. Raw number concentrations were adjusted to 2nd floor monitor equivalent values as an arbitrary reference following procedures

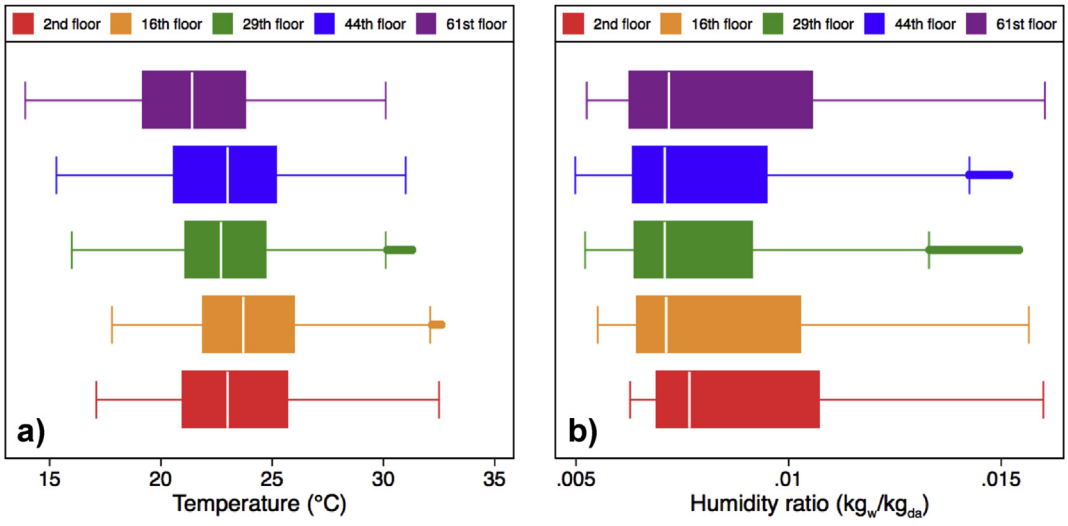


**Fig. 1.** Box plots of (a) temperature and (b) humidity ratio data measured on each of the five floors.

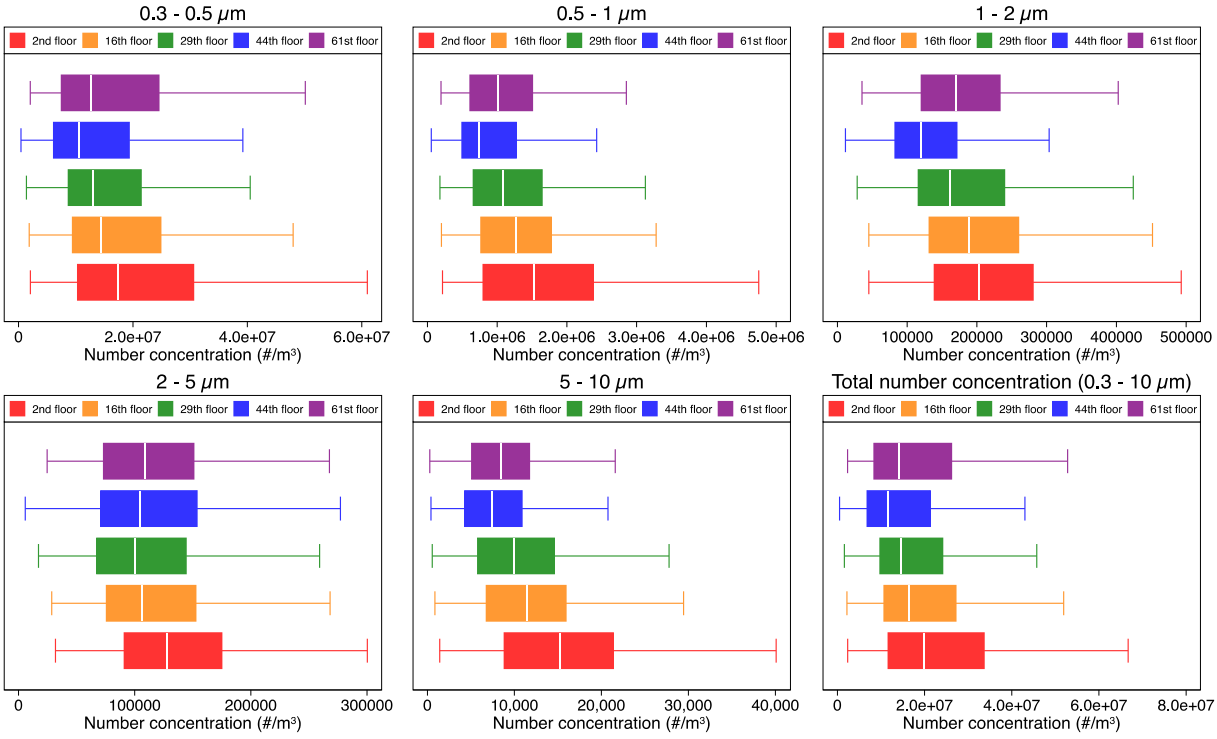


**Fig. 2.** Box plots of size-resolved particle number concentration data measured on each of the five floors. Bins include: 0.3–0.5 μm, 0.5–1 μm, 1–2 μm, 2–5 μm, 5–10 μm, and total number concentrations (0.3–10 μm). Outliers are excluded for graphical clarity.

described in the SI. Number concentrations for each particle size bin measured on the 16th floor and above were consistently lower than those measured on the 2nd floor, with reasonably similar trends for most particle size bins (albeit with some deviations, particularly in the 61st floor measurements). The lowest number concentrations for most particle sizes along the height of the building were observed on the 44th floor, as median concentrations in the 0.5–1 μm and 5–10 μm size ranges were both ~51% lower than the median concentrations on the 2nd floor. The smallest decreases in number concentrations along the height of the building were observed for particles in the 2–5 μm size range, with median decreases between measurements on the 16th floor and above and the 2nd floor ranging from ~15% to ~21%.

### 3.2.2. Estimates of $PM_1$, $PM_{2.5}$, and $PM_{10}$ mass concentrations

Fig. 3 shows box plots of estimates of $PM_1$, $PM_{2.5}$, and $PM_{10}$ mass concentrations made using number concentrations measured on each of the five floors, with outliers excluded for clarity. Figs. S21, S22, and S23 show full weeklong time-series data. Again, raw concentrations were adjusted to 2nd floor monitor equivalent values as an arbitrary reference. Estimates of PM mass concentrations were strongly correlated with number concentrations from the closest corresponding size bins (i.e., Spearman rank correlation coefficients were greater than 0.9 between $PM_1$ and the 0.3–1 μm bins; greater than 0.8 between $PM_{2.5}$ and the 0.3–2 μm bins; and greater than 0.85 between PM10 and the 2–10 μm bins).

The median (and mean) $PM_1$, $PM_{2.5}$, and $PM_{10}$ concentrations estimated from number measurements in the 2nd floor outdoor air intake as a near-ground reference were ~1.3 (~1.5) μg/m$^3$, ~2.2 (~2.3) μg/m$^3$, and ~9.3 (~10.6) μg/m$^3$, respectively, throughout the week, which are surprisingly low for an urban environment such as Chicago. However, the average daily $PM_{2.5}$ concentration measured at the nearest ambient regulatory monitor (#17-031-0057, 1745 N Springfield Ave, Chicago, IL, ~9 km away) was only 2.8 μg/m$^3$ during the measurement campaign [64]. For comparison, the average daily $PM_{2.5}$ concentration for the year 2017 measured at the same regulatory monitor was ~8.6 μg/m$^3$. Although this presents only a limited

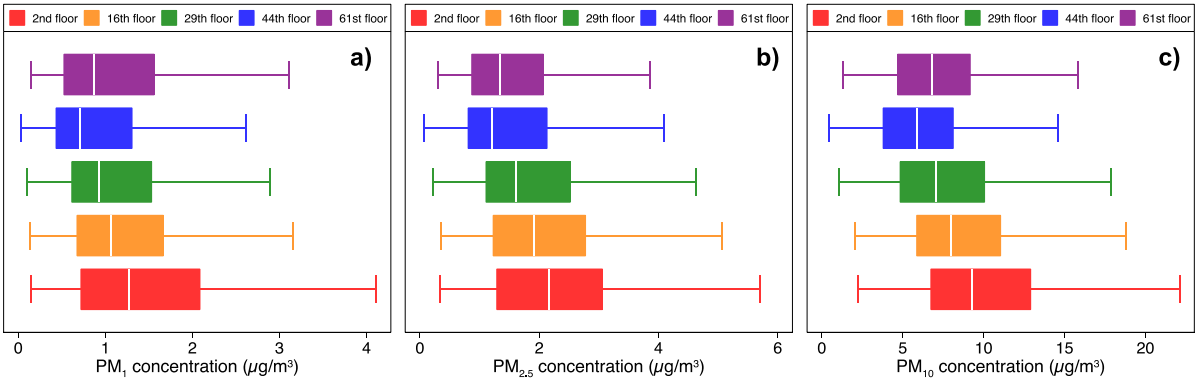


**Fig. 3.** Box plots of estimates of (a) $PM_1$, (b) $PM_{2.5}$, and (c) $PM_{10}$ mass concentrations made from number concentrations measured on each of the five floors. Outliers are excluded for graphical clarity. The PM mass concentrations are estimates made assuming spherical shape and density = 1.5 g/cm$^3$. No mass below 0.3 μm is counted, so mass concentrations are likely underestimated.

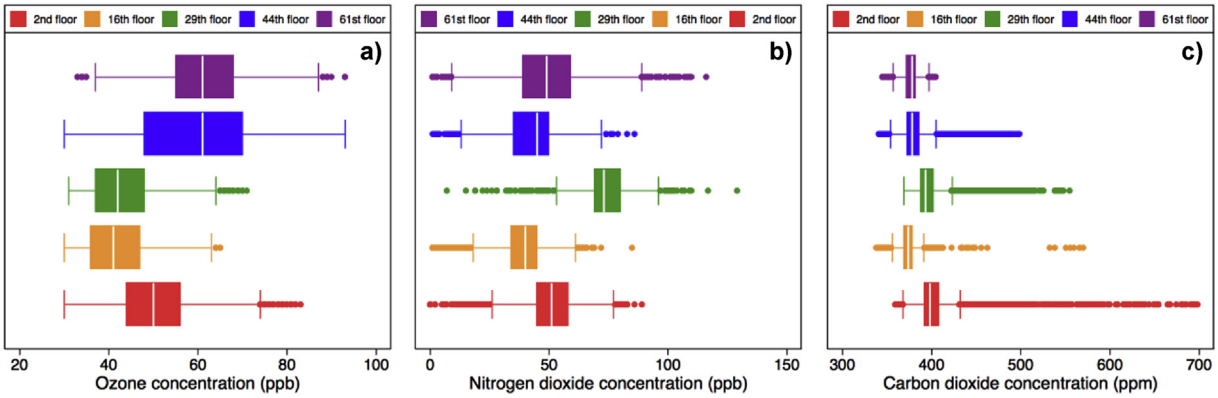


**Fig. 4.** Box plots of (a) ozone ($O_3$), (b) nitrogen dioxide ($NO_2$), and (c) carbon dioxide ($CO_2$) concentration data measured on each of the five floors.

comparison, it demonstrates that the field campaign happened to occur during a period of relatively low ambient PM concentrations.

The average $PM_1$ concentration was estimated to be ~18.4%, ~24.8%, ~34.5%, and ~23.7% lower on the 16th, 29th, 44th, and 61st floors compared to the 2nd floor, respectively, suggesting a fairly consistent trend of $PM_1$ concentrations decreasing with building height. Similarly, the average $PM_{2.5}$ concentration was estimated to be ~10.4%, ~18.0%, ~30.3%, and ~31.7% lower on the 16th, 29th, 44th, and 61st floors compared to the 2nd floor, respectively. All $PM_1$ and $PM_{2.5}$ comparisons were statistically significant except for the comparison between $PM_{2.5}$ concentrations measured on the 44th and 61st floors. The trend for both $PM_1$ and $PM_{2.5}$ was nearly linear from floors 2 through 44, with a deviation in the open-air 61st floor location. The $PM_1$ and $PM_{2.5}$ concentration dispersion data are reasonably consistent with prior ambient measurements [37,38].

The average $PM_{10}$ concentration was estimated to be ~12.9%, ~32.4%, and ~31.5% lower on the 29th, 44th, and 61st floors compared to the 2nd floor, respectively, but actually ~15.8% higher on the 16th floor compared to the 2nd floor (although the median $PM_{10}$ concentration on the 16th floor is still lower than the 2nd floor as shown in Fig. 3c). All $PM_{10}$ comparisons were statistically significant (Table 1). This inconsistent trend at the lower levels may be suggestive of local ground sources with greater dilution occurring at higher elevations. Interestingly, the standard deviation of $PM_{10}$ concentrations was largest

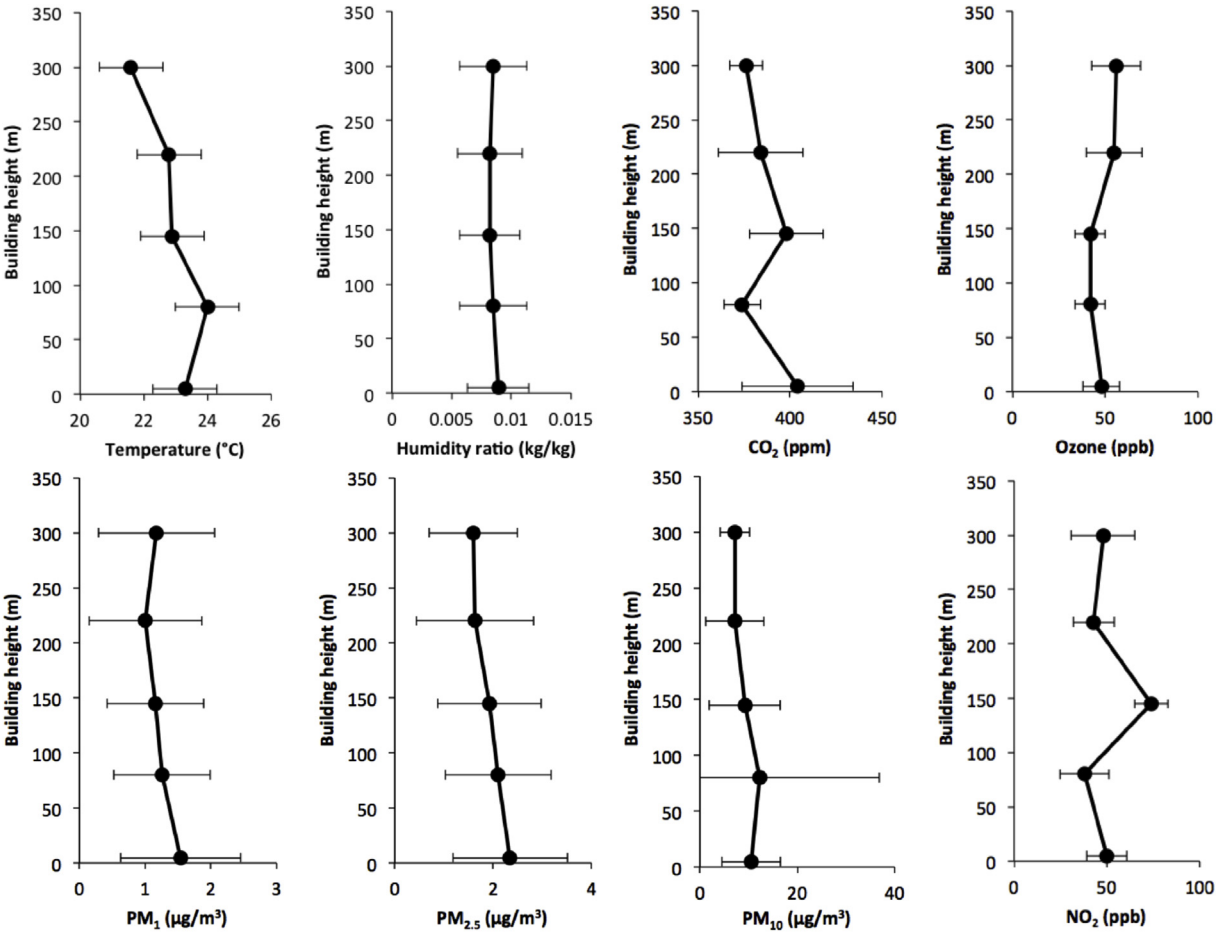


**Fig. 5.** Average ( ± standard deviation) of the $CO_2$, $O_3$, $NO_2$, $PM_1$, $PM_{2.5}$, and $PM_{10}$ concentrations and the air temperature and humidity ratios measured (or estimated) during the weeklong field campaign plotted against the approximate floor height of the test building.

**Table 1**
Significance testing on paired data sets of each parameter compared between each floor using nonparametric Wilcoxon signed-rank tests.

| | Temp. | RH | Humidity Ratio | $CO_2$ | $O_3$ | $PM_1$ | $PM_{2.5}$ | $PM_{10}$ | $NO_2$ |
|---|---|---|---|---|---|---|---|---|---|
| Sample size, n[a] | 9928 | 9928 | 9928 | 10089 | 9901 | 4959 | 4959 | 4959 | 8131 |
| Adj. p-value threshold | $5.17 \times 10^{-6}$ | $5.17 \times 10^{-6}$ | $5.17 \times 10^{-6}$ | $5.08 \times 10^{-6}$ | $5.18 \times 10^{-6}$ | $1.03 \times 10^{-5}$ | $1.03 \times 10^{-5}$ | $1.03 \times 10^{-5}$ | $6.31 \times 10^{-6}$ |
| 2nd and 16th | *** | *** | *** | *** | *** | *** | ** | *** | *** |
| 2nd and 29th | *** | *** | *** | ** | *** | *** | *** | *** | *** |
| 2nd and 44th | *** | *** | *** | *** | *** | *** | *** | *** | *** |
| 2nd and 61st | *** | *** | *** | *** | *** | *** | *** | *** | * |
| 16th and 29th | *** | *** | *** | *** | * | ** | ** | *** | *** |
| 16th and 44th | *** | *** | *** | *** | *** | *** | *** | *** | *** |
| 16th and 61st | *** | *** | n.s. | *** | *** | ** | *** | *** | *** |
| 29th and 44th | ** | ** | ** | *** | *** | ** | *** | ** | *** |
| 29th and 61st | *** | *** | ** | *** | *** | * | *** | ** | *** |
| 44th and 61st | *** | *** | *** | ** | * | *** | n.s. | ** | ** |

***$p < 10^{-250}$.
**$10^{-250} < p < 10^{-100}$.
* $10^{-100} < p <$ threshold.
n.s. = not significant.
[a] Comparisons are made using 1-min or 2-min interval data as dictated by each instrument. Only those cells with bold text failed to reach statistical significance based on a threshold p-value that is adjusted for sample size.

on the 16th floor, which means that there were periodically very high $PM_{10}$ concentrations measured on the 16th floor and suggests an influence from nearby transient $PM_{10}$ sources around this height.

### 3.3. Gaseous pollutants: $O_3$, $NO_2$, and $CO_2$

Fig. 4 shows box plots of the $O_3$, $NO_2$, and $CO_2$ concentrations measured on the five floors and Figs. S24, S25, and S26 show the full weeklong time-series data. For $O_3$, each data point was adjusted to the federal equivalent method (FEM) reference instrument (2B Technologies Model 211) following calibration procedures described in the SI. Only data above the highest measured LOD for the SM50 instruments (~30 ppb) are shown, as varying LODs make it impossible to compare null values with actual values recorded at concentrations lower than ~30 ppb. For $NO_2$ and $CO_2$, each data point was adjusted to 2nd floor monitor equivalent values as an arbitrary reference. All observed differences in $O_3$, $NO_2$, and $CO_2$ concentrations between floors were statistically significant (Table 1).

The average $O_3$ concentration across all floors (when limiting to data above an LOD of ~30 ppb) was ~48 ppb throughout the week, with a maximum of ~122 ppb. The measured $O_3$ concentrations were similar to the average daily $O_3$ concentration of ~46 ppb measured at the three nearest ambient regulatory monitors (#17-031-0003 6545 W Hurlbut St; #17-031-0032, 3300 E Cheltenham Pl; and #17-031-0076, 7801 Lawndale; each ~15–20 km away) during the field campaign [64]. Further, historical records of $O_3$ concentrations measured by these same regulatory monitors suggest that hourly $O_3$ concentrations are typically below 30 ppb during periods in late June approximately 20–30% of the time [64]; a similar fraction of data points were excluded for being below the 30 ppb LOD on most floors in our data set as well.

The average $O_3$ concentration above this LOD was ~11.9% and ~11.3% lower on the 16th and 29th floors compared to the 2nd floor, respectively, but ~16.0% and ~18.0% higher on the 44th and 61st floors compared to the 2nd floor, respectively. This inconsistent vertical trend in $O_3$ concentrations is not unlike the limited data from aircraft measurements reported in the literature reviewed in Section 1, in which concentrations first decrease and then increase with elevation [32]. This may be due in part to titration of $O_3$ by NO from ground-level tailpipe emission sources, which might not reach the higher elevations or might be diluted and/or reacted by the time air masses reached higher elevations. We should also note that we have somewhat lower confidence in these ozone concentration measurements based on the potential for calibration factors to vary with temperature, relative humidity, and interference by other compounds that have not been captured in our calibration procedures or field measurements [52].

The average $NO_2$ concentration across all floors (when reporting data using the 2nd floor monitor as an arbitrary reference) was ~50 ppb throughout the week, with a maximum of ~129 ppb encountered on the 29th floor. Conversely, the average daily $NO_2$ concentration measured by the nearest regulatory monitor (#17-031-0063, 321 S Franklin, Chicago, IL) was only 21 ppb. Because of the close proximity of the test building to the nearest $NO_2$ regulatory monitor, reasons for this discrepancy are most likely attributed to artifacts in the monitoring devices and issues that prevented a true calibration against research grade equipment. For example, Section 1.2.4 in the SI (including Fig. S15) clearly shows a positive offset of ~30–50 ppb for the Aeroqual S500 monitors compared to the 2B Technologies Model 405 monitor that unfortunately could not be systematically accounted for in data processing. Despite this offset issue, data from the S500 $NO_2$ monitors should still yield meaningful comparisons on a relative basis (i.e., when calibrated against each other). Using these data, the average $NO_2$ concentration was ~25.3% lower on the 16th floor, ~47.0% higher on the 29th floor, ~15.1% lower on the 44th floor, and ~5.3% lower on the 61st floor, each compared to the 2nd floor. Reasons for this inconsistent trend are not clear, but it is worth noting that, similar to the $O_3$ measurements, we also have somewhat lower confidence in these $NO_2$ concentration measurements based on the potential for calibration factors to vary with temperature, relative humidity, and interference by other compounds that have not been captured in our calibration procedures or field measurements [52].

Finally, the average $CO_2$ concentration across all floors was ~387 ppm throughout the week, with a maximum of ~700 ppm observed on the 2nd floor. The average $CO_2$ concentration was ~7.6%, ~1.5%, ~4.9%, and ~6.9% lower on the 16th, 29th, 44th, and 61st floors compared to the 2nd floor, respectively. These relative differences correspond to average absolute differences of ~30 ppm, ~6 ppm, ~20 ppm, and ~28 ppm, respectively. There was no consistent linear trend in average $CO_2$ concentrations across all elevations, although once again, concentrations were consistently lower on all floors above the 2nd floor, suggesting dilution or dispersion of ground-level sources at higher floors.

### 3.4. Diurnal patterns between floors

Fig. 6 shows box plots (excluding outliers) of the diurnal variations

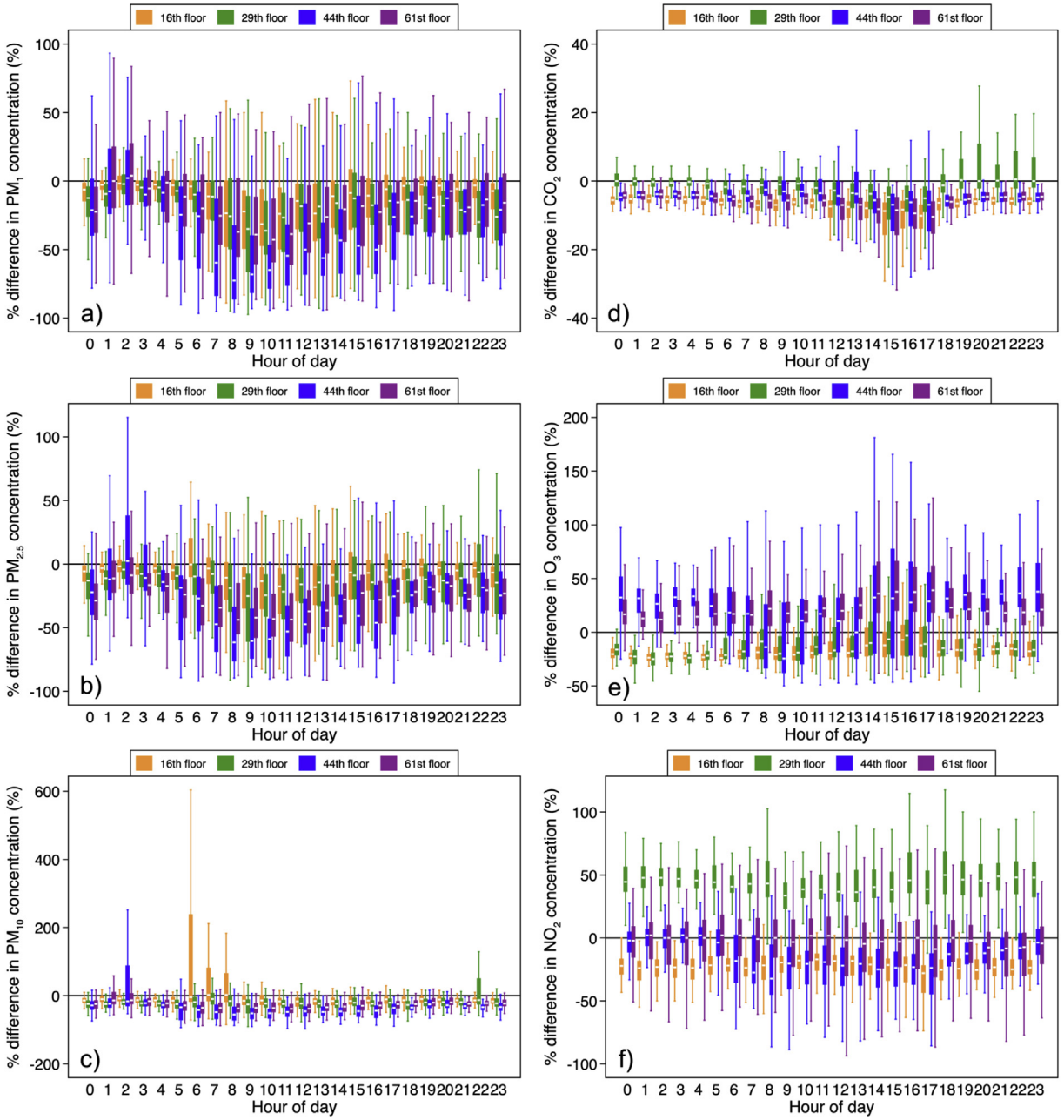


**Fig. 6.** Diurnal patterns of the relative differences in (a) $PM_1$, (b) $PM_{2.5}$, (c) $PM_{10}$, (d) $CO_2$, (e) $O_3$, and (f) $NO_2$ concentrations measured on the 16th, 29th, 44th, and 61st floors compared to the 2nd floor (i.e., nth floor values minus the 2nd floor values). Outliers are excluded for graphical clarity.

in relative differences in $PM_1$, $PM_{2.5}$, $PM_{10}$, $CO_2$, $O_3$, and $NO_2$ concentrations measured on the 16th, 29th, 44th, and 61st floors compared to the 2nd floor. Relative differences are calculated as the simultaneous nth floor values minus the simultaneous 2nd floor values, divided by the simultaneous 2nd floor values. Values are reported for each of the 24 h of each day, aggregated across all days of the measurement campaign. The maximum differences in estimates of $PM_1$ and $PM_{2.5}$ concentrations tended to occur in the morning and midday from ~7 a.m. to ~2 p.m., while smaller and relatively consistent differences were observed during other time periods. Some large peaks observed around 5 a.m.–8 a.m. drove most of the differences in $PM_{10}$ concentrations, particularly on the 16th floor. A few other transient peaks in estimates of $PM_{10}$ concentrations were also seen at other hours on the 29th and 44th floors, suggesting some highly localized sources or perhaps even resuspension of settled dust by the presence of maintenance personnel within the outdoor intake areas (although this could not be confirmed). The maximum differences in $CO_2$ concentrations were observed in the late afternoons from ~2 p.m. to ~5 p.m., suggesting likely contributions from vehicle sources as traffic starts to increase in the area. There were no clear diurnal patterns in the differences in observed $O_3$ and $NO_2$ concentrations other than a mild increase in differences in $O_3$ concentrations at higher elevations in the late afternoons. Combined, these data generally suggest that variations along the building's height are reasonably consistent throughout the day, albeit with some periodic pollutant-specific deviations.

Similarly, Fig. 7 shows box plots (excluding outliers) of the diurnal variations in relative differences in temperature and relative humidity measured on the 16th, 29th, 44th, and 61st floors compared to the 2nd floor. The largest differences in temperature and, to a greater extent, humidity ratio, tended to occur in the late afternoons and early evenings (e.g., ~2–~5 p.m.), with some periodically large deviations among certain floors at other times of day. For example, there were

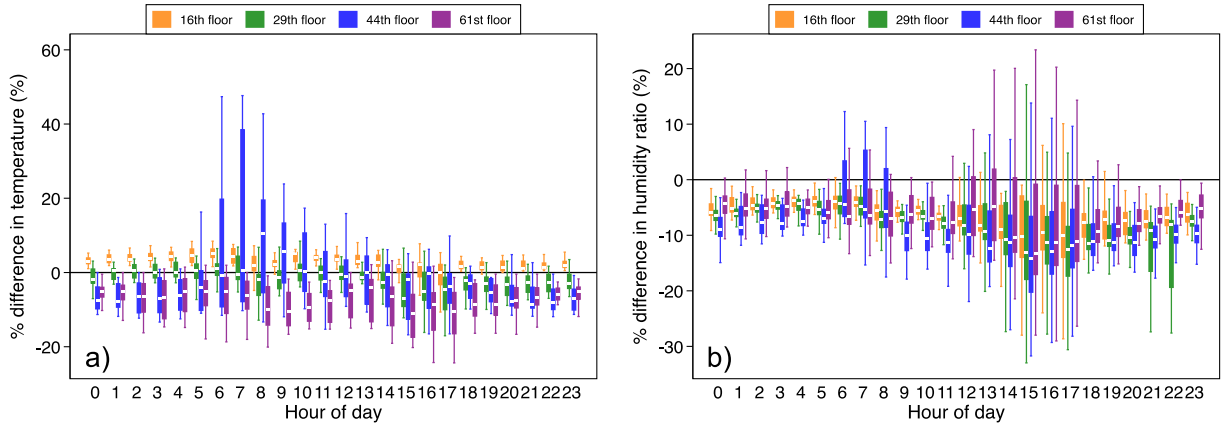


**Fig. 7.** Diurnal patterns of the relative differences in (a) temperature and (b) humidity ratio measured on the 16th, 29th, 44th, and 61st floors compared to the 2nd floor (i.e., nth floor values minus the 2nd floor values). Outliers are excluded for graphical clarity.

large increases in temperatures on the 44th floor in the early morning hours (~6–~8 a.m.) and large decreases in humidity ratios on the 29th floor at night (~8–~10 p.m.), likely caused by temporary anthropogenic sources, perhaps including operation of HVAC systems in nearby buildings, changes in vehicle traffic patterns [65], or other common street canyon effects [24–26].

### 3.5. Potential drivers of variations in the measured data

The obtained wind speed and wind direction data from the Weather Underground Personal Weather Station Network [44] were combined with building height to investigate the potential drivers of the observed variations in measured (or estimated) parameters. The average (± standard deviation) hourly wind speed and wind direction near the measurement site were 2.5 (± 1.3) m/s and 193° (± 47°) (i.e., from the south-southwest), respectively (Fig. 8). The most prevalent wind direction was ~200°–~250° (i.e., predominantly from the southwest), which would be expected to transport traffic-related pollutants from the heavily trafficked I-90/94 and I-290 interstates toward the building located in downtown Chicago, IL. Note that Lake Michigan is to the east of the measurement site. There was minimal rainfall during the sampling period, with ~1.2 cm falling between 6:30 a.m. and 11:00 p.m. on June 23 and another ~0.4 cm falling between 12:30 p.m. and midnight on June 28.

Spearman rank correlation coefficients were calculated using hourly

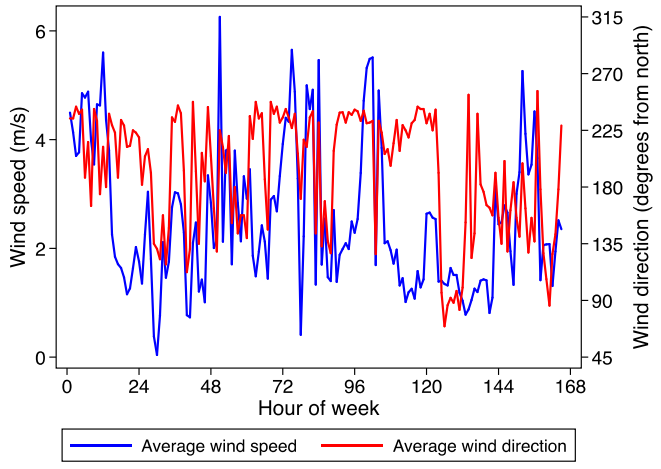


**Fig. 8.** Hourly average wind speed and direction taken from a nearby Weather Underground Personal Weather Station Network [60]. Wind direction is measured as 'degrees from north' (i.e., 0 = north; 90 = east; 180 = south; 270 = west).

**Table 2**
Spearman rank correlation coefficients and significance testing between measured (or estimated) parameters and floor height, wind direction, and wind speed.

| Parameter | Spearman rank correlation coefficients (p-value) | | |
|---|---|---|---|
| | Floor height | Wind direction | Wind speed |
| Temperature | −0.186 (< 0.0001) | −0.202 (< 0.0001) | 0.248 (< 0.0001) |
| Humidity ratio | −0.120 (0.0006) | −0.191 (< 0.0001) | 0.060 (0.084) |
| $PM_1$ | −0.195 (< 0.0001) | −0.174 (< 0.0001) | −0.065 (0.062) |
| $PM_{2.5}$ | −0.195 (< 0.0001) | −0.174 (< 0.0001) | −0.065 (0.062) |
| $PM_{10}$ | −0.275 (< 0.0001) | −0.220 (< 0.0001) | −0.082 (0.019) |
| $CO_2$ | −0.358 (< 0.0001) | 0.086 (0.013) | −0.143 (< 0.0001) |
| $O_3$ | 0.362 (< 0.0001) | −0.144 (0.0001) | 0.025 (0.490) |
| $NO_2$ | −0.004 (0.914) | 0.179 (< 0.0001) | 0.038 (0.325) |

averages of each measured parameter as the dependent variable and building height, hourly average wind speed, and hourly average wind direction as independent variables (Table 2). Results show that the variable that was most strongly correlated with most of the measured (or estimated) pollutant concentrations was floor height, with the highest Spearman rank correlation coefficients calculated for hourly average $PM_1$, $PM_{2.5}$, $PM_{10}$, $O_3$, and $CO_2$ concentrations in particular. Spearman rank correlation coefficients were negative for all of these pollutants, suggesting a decreasing trend in concentration with building height, except $O_3$, which showed an increasing trend in concentration with building height. Moreover, each of these comparisons with building height was statistically significant ($p < 0.0001$), but relatively weak (i.e., Spearman rank correlation coefficients with building height ranging from −0.18 to −0.36). The comparison between $NO_2$ concentrations and building height was not significant; however, wind direction was positively correlated with measured $NO_2$ concentrations, which suggests $NO_2$ concentrations were higher when the prevailing wind direction was from the southwest (supporting the hypothesized transport of vehicular $NO_2$ emissions).

Building height was also significantly correlated with temperature and humidity ratio, but wind direction was more strongly correlated with both parameters. Wind speed showed the strongest association with temperature, but was weakest for humidity ratio. These data demonstrate that the majority of floor-by-floor comparisons shown

previously are robust to the inclusion of other local meteorological factors, and although prevailing environmental conditions in the area had an influence on some of the observed variations in the measured parameters, building height had the strongest correlations with all but one measured pollutant ($NO_2$) and was also correlated with temperature and humidity ratio. However, we should note that correlation coefficients calculated for comparisons among individual variables were not particularly high (i.e., always less than 0.37), suggesting that even the statistically significant relationships were fairly weak.

Taken together, these pilot study data add valuable contributions to the existing limited numbers of experimental investigations as well as numerous modeling and wind tunnel investigations on pollutant dispersion and local environmental conditions in urban environments within the context of tall buildings. These pilot data also suggest the following implications for the design and operation of tall buildings: (1) the dry bulb temperature lapse rate of a building can deviate from the linear Standard Lapse Rate assumption during some periods, which may need to be accounted for in HVAC design and energy simulation; (2) concentrations of some ambient pollutants or constituents, especially measurements of PM number concentrations and estimates of PM mass concentrations, and, to a lesser extent, $CO_2$, showed strong signatures of ground-level emissions that become dispersed or diluted at higher floors, which may need to be accounted for in designing and operating ventilation and particle filtration systems; and (3) concentrations of $O_3$ were clearly highest at the highest elevations of the building, which may also need to be considered in the design and operation of ventilation and gas-phase filtration systems.

## 4. Conclusions

To our knowledge, this data set represents the first known measurements of the vertical variation in concentrations of several health relevant outdoor pollutants and climatically relevant outdoor environmental parameters in outdoor air intakes along the height of a tall building in a major metropolitan area. In general, the arithmetic mean values of most measured parameters tended to decrease with building height, albeit with some exceptions. The magnitude of measured differences among floors was statistically significant but typically small for most parameters (i.e., less than 10% for temperature, relative humidity, humidity ratio, and $CO_2$) but larger for others (i.e., up to a maximum decrease of ~32%, with averages consistently decreasing with floor height, for estimates of $PM_1$ and $PM_{2.5}$ concentrations). Variations in other parameters such as $PM_{10}$, $O_3$, and $NO_2$ concentrations were less consistent and varied in magnitude. Given some of the relatively large magnitudes of differences in measured values observed herein, we recommend that additional measurements be made in other tall and super-tall buildings in other climate zones and geographic regions to better understand how and why pollutant concentrations vary with elevation at scales that are relevant to occupants of these building types.

## Acknowledgments

We would like to acknowledge the Council on Tall Buildings and Urban Habitat (CTBUH) and funding sponsor Taipei Financial Center Corporation for their generous financial support of this project. We are also extremely grateful to the anonymous building ownership and facilities staff members that made these measurements possible.

## Appendix A. Supplementary data

Supplementary data related to this article can be found at http://dx.doi.org/10.1016/j.buildenv.2018.04.031.

## References

[1] C.A. Pope, R.T. Burnett, M.J. Thun, E.E. Calle, D. Krewski, K. Ito, G.D. Thurston, Lung cancer, cardiopulmonary mortality, and long-term exposure to fine particulate air pollution, JAMA, J. Am. Med. Assoc. 287 (2002) 1132–1141.
[2] C.A. Pope, D.W. Dockery, Health effects of fine particulate air pollution: lines that connect, J. Air Waste Manag. Assoc. 56 (2006) 709–742.
[3] K.A. Miller, D.S. Siscovick, L. Sheppard, K. Shepherd, J.H. Sullivan, G.L. Anderson, J.D. Kaufman, Long-term exposure to air pollution and incidence of cardiovascular events in women, N. Engl. J. Med. 356 (2007) 447–458, http://dx.doi.org/10.1056/NEJMoa054409.
[4] R.D. Brook, S. Rajagopalan, C.A. Pope, J.R. Brook, A. Bhatnagar, A.V. Diez-Roux, F. Holguin, Y. Hong, R.V. Luepker, M.A. Mittleman, A. Peters, D. Siscovick, S.C. Smith, L. Whitsel, J.D. Kaufman, Particulate matter air pollution and cardiovascular disease, Circulation 121 (2010) 2331–2378, http://dx.doi.org/10.1161/CIR.0b013e3181dbece1.
[5] U.S. EPA, Integrated Science Assessment for Oxides of Nitrogen – Health Criteria, National Center for Environmental Assessment-rtp Division, Office of Research and Development, U.S. Environmental Protection Agency, Research Triangle Park, NC, 2016.
[6] US EPA, Integrated Science Assessment for Particulate Matter, National Center for Environmental Assessment, Research Triangle Park, NC, 2009.
[7] S.C. Anenberg, L.W. Horowitz, D.Q. Tong, J.J. West, An estimate of the global burden of anthropogenic ozone and fine particulate matter on premature human mortality using atmospheric modeling, Environ. Health Perspect. 118 (2010) 1189–1195, http://dx.doi.org/10.1289/ehp.0901220.
[8] L. Han, W. Zhou, W. Li, Increasing impact of urban fine particles (PM2.5) on areas surrounding Chinese cities, Sci. Rep. 5 (2015), http://dx.doi.org/10.1038/srep12467.
[9] A. van Donkelaar, R.V. Martin, M. Brauer, B.L. Boys, Use of satellite observations for long-term exposure assessment of global concentrations of fine particulate matter, Environ. Health Perspect. (2014), http://dx.doi.org/10.1289/ehp.1408646.
[10] R. Vingarzan, A review of surface ozone background levels and trends, Atmos. Environ. 38 (2004) 3431–3442, http://dx.doi.org/10.1016/j.atmosenv.2004.03.030.
[11] US EPA, 40 CFR Appendix E to Part 58, Probe and Monitoring Path Siting Criteria for Ambient Air Quality Monitoring, (2012).
[12] N.E. Klepeis, W.C. Nelson, W.R. Ott, J.P. Robinson, A.M. Tsang, P. Switzer, J.V. Behar, S.C. Hern, W.H. Engelmann, The National Human Activity Pattern Survey (NHAPS): a resource for assessing exposure to environmental pollutants, J. Expo. Anal. Environ. Epidemiol. 11 (2001) 231–252, http://dx.doi.org/10.1038/sj.jea.7500165.
[13] C.J. Weschler, New Directions: ozone-initiated reaction products indoors may be more harmful than ozone itself, Atmos. Environ. 38 (2004) 5715–5716, http://dx.doi.org/10.1016/j.atmosenv.2004.08.001.
[14] C.J. Weschler, Ozone's impact on public health: contributions from indoor exposures to ozone and products of ozone-initiated chemistry, Environ. Health Perspect. 114 (2006) 1489–1496, http://dx.doi.org/10.1289/ehp.9256.
[15] C.J. Weschler, Ozone in indoor environments: concentration and chemistry, Indoor Air 10 (2000) 269–288, http://dx.doi.org/10.1034/j.1600-0668.2000.010004269.x.
[16] B. Stephens, E.T. Gall, J.A. Siegel, Measuring the penetration of ambient ozone into residential buildings, Environ. Sci. Technol. 46 (2012) 929–936, http://dx.doi.org/10.1021/es2028795.
[17] Q.Y. Meng, B.J. Turpin, L. Korn, C.P. Weisel, M. Morandi, S. Colome, J. Zhang, T. Stock, D. Spektor, A. Winer, L. Zhang, J.H. Lee, R. Giovanetti, W. Cui, J. Kwon, S. Alimokhtari, D. Shendell, J. Jones, C. Farrar, S. Maberti, Influence of ambient (outdoor) sources on residential indoor and personal PM2.5 concentrations: analyses of RIOPA data, J. Expo. Anal. Environ. Epidemiol. 15 (2005) 17–28, http://dx.doi.org/10.1038/sj.jea.7500378.
[18] J. Kearney, L. Wallace, M. MacNeill, X. Xu, K. VanRyswyk, H. You, R. Kulka, A.J. Wheeler, Residential indoor and outdoor ultrafine particles in Windsor, Ontario, Atmos. Environ. 45 (2011) 7583–7593, http://dx.doi.org/10.1016/j.atmosenv.2010.11.002.
[19] B. Stephens, J.A. Siegel, Penetration of ambient submicron particles into single-family residences and associations with building characteristics, Indoor Air 22 (2012) 501–513, http://dx.doi.org/10.1111/j.1600-0668.2012.00779.x.
[20] Z. El Orch, B. Stephens, M.S. Waring, Predictions and determinants of size-resolved particle infiltration factors in single-family homes in the U.S, Build. Environ. 74 (2014) 106–118, http://dx.doi.org/10.1016/j.buildenv.2014.01.006.
[21] W.J. Riley, T.E. McKone, A.C.K. Lai, W.W. Nazaroff, Indoor particulate matter of outdoor origin: importance of size-dependent removal mechanisms, Environ. Sci. Technol. 36 (2002) 200–207, http://dx.doi.org/10.1021/es010723y.
[22] T.N. Quang, C. He, L. Morawska, L.D. Knibbs, M. Falk, Vertical particle concentration profiles around urban office buildings, Atmos. Chem. Phys. 12 (2012) 5017–5030, http://dx.doi.org/10.5194/acp-12-5017-2012.
[23] C.-D. Wu, P. MacNaughton, S. Melly, K. Lane, G. Adamkiewicz, J.L. Durant, D. Brugge, J.D. Spengler, Mapping the vertical distribution of population and particulate air pollution in a near-highway urban neighborhood: implications for exposure assessment, J. Expo. Sci. Environ. Epidemiol. 24 (2014) 297–304, http://dx.doi.org/10.1038/jes.2013.64.
[24] K. Ahmad, M. Khare, K.K. Chaudhry, Wind tunnel simulation studies on dispersion at urban street canyons and intersections—a review, J. Wind Eng. Ind. Aerod. 93 (2005) 697–717, http://dx.doi.org/10.1016/j.jweia.2005.04.002.
[25] J. Hang, Y. Li, M. Sandberg, R. Buccolieri, S. Di Sabatino, The influence of building

height variability on pollutant dispersion and pedestrian ventilation in idealized high-rise urban areas, Build. Environ. 56 (2012) 346–360, http://dx.doi.org/10.1016/j.buildenv.2012.03.023.
[26] Y. Tominaga, T. Stathopoulos, CFD modeling of pollution dispersion in a street canyon: comparison between LES and RANS, J. Wind Eng. Ind. Aerod. 99 (2011) 340–348, http://dx.doi.org/10.1016/j.jweia.2010.12.005.
[27] N.J. Duijm, Dispersion over complex terrain: wind-tunnel modelling and analysis techniques, Atmos. Environ. 30 (1996) 2839–2852, http://dx.doi.org/10.1016/1352-2310(95)00344-4.
[28] A. Mfula, V. Kukadia, R. Griffiths, D. Hall, Wind tunnel modelling of urban building exposure to outdoor pollution, Atmos. Environ. 39 (2005) 2737–2745, http://dx.doi.org/10.1016/j.atmosenv.2004.07.040.
[29] I. Mavroidis, R. Griffiths, Local characteristics of atmospheric dispersion within building arrays, Atmos. Environ. 35 (2001) 2941–2954, http://dx.doi.org/10.1016/S1352-2310(00)00456-8.
[30] G. Villena, J. Kleffmann, R. Kurtenbach, P. Wiesen, E. Lissi, M.A. Rubio, G. Croxatto, B. Rappenglück, Vertical gradients of HONO, NOx and O3 in Santiago de Chile, Atmos. Environ. 45 (2011) 3867–3873, http://dx.doi.org/10.1016/j.atmosenv.2011.01.073.
[31] R.A. Mccormick, D.M. Baulch, The variation with height of the dust loading over a city as determined from the atmospheric turbidity, J. Air Pollut. Contr. Assoc. 12 (1962) 492–496, http://dx.doi.org/10.1080/00022470.1962.10468119.
[32] CTBUH, CTBUH Height Criteria for Measuring & Defining Tall Buildings, Council on Tall Buildings and Urban Habitat (CTBUH), n.d. http://www.ctbuh.org/LinkClick.aspx?fileticket=zvoB1S4nMug=.
[33] J. Zhang, S.T. Rao, The role of vertical mixing in the temporal evolution of ground-level ozone concentrations, J. Appl. Meteorol. 38 (1999) 1674–1691, http://dx.doi.org/10.1175/1520-0450(1999)038<1674:TROVMI>2.0.CO;2.
[34] H.A. Flocas, V.D. Assimakopoulos, C.G. Helmis, H. Güsten, VOC and $O_3$ distributions over the densely populated area of greater athens, Greece, J. Appl. Meteorol. 42 (2003) 1799–1810, http://dx.doi.org/10.1175/1520-0450(2003)042<1799:VAODOT>2.0.CO;2.
[35] C. Du, S. Liu, X. Yu, X. Li, C. Chen, Y. Peng, Y. Dong, Z. Dong, F. Wang, Urban boundary layer height characteristics and relationship with particulate matter mass concentrations in Xi'an, Central China, Aerosol Air Qual. Res (2013), http://dx.doi.org/10.4209/aaqr.2012.10.0274.
[36] J. Song, Z.-H. Wang, Diurnal changes in urban boundary layer environment induced by urban greening, Environ. Res. Lett. 11 (2016) 114018, , http://dx.doi.org/10.1088/1748-9326/11/11/114018.
[37] C. Li, J. Fu, G. Sheng, X. Bi, Y. Hao, X. Wang, B. Mai, Vertical distribution of PAHs in the indoor and outdoor PM2.5 in Guangzhou, China, Build. Environ. 40 (2005) 329–341, http://dx.doi.org/10.1016/j.buildenv.2004.05.015.
[38] L. Chan, W. Kwok, Vertical dispersion of suspended particulates in urban area of Hong Kong, Atmos. Environ. 34 (2000) 4403–4412, http://dx.doi.org/10.1016/S1352-2310(00)00181-3.
[39] R. Panczak, B. Galobardes, A. Spoerri, M. Zwahlen, M. Egger, High life in the sky? Mortality by floor of residence in Switzerland, Eur. J. Epidemiol. 28 (2013) 453–462, http://dx.doi.org/10.1007/s10654-013-9809-8.
[40] M.J. Mendell, Q. Lei-Gomez, A.G. Mirer, O. Seppnen, G. Brunner, Risk factors in heating, ventilating, and air-conditioning systems for occupant symptoms in US office buildings: the US EPA BASE study, Indoor Air 18 (2008) 301–316, http://dx.doi.org/10.1111/j.1600-0668.2008.00531.x.
[41] CTBUH, Tall Buildings in Numbers: 2017 Year in Review, Skyscraper Cent, 2017, http://www.skyscrapercenter.com/year-in-review/2017.
[42] W.R. Chan, B.C. Singer, Measurement-based Evaluation of Installed Filtration System Performance in Single-family Homes, Lawrence Berkeley National Laboratory, Berkeley, CA, 2014.
[43] S. Shen, P.A. Jaques, Y. Zhu, M.D. Geller, C. Sioutas, Evaluation of the SMPS–APS system as a continuous monitor for measuring PM2.5, PM10 and coarse (PM2.5 − 10) concentrations, Atmos. Environ. 36 (2002) 3939–3950, http://dx.doi.org/10.1016/S1352-2310(02)00330-8.
[44] A. Khlystov, C. Stanier, S.N. Pandis, An algorithm for combining electrical mobility and aerodynamic size distributions data when measuring ambient aerosol, Aerosol. Sci. Technol. 38 (2004) 229–238, http://dx.doi.org/10.1080/02786820390229543.
[45] W.R. Chan, F. Noris, Side-by-Side Comparison of Particle Count and Mass Concentration Measurements in a Residence, Lawrence Berkeley National Laboratory, Berkeley, CA, 2011.
[46] G. Buonanno, M. Dell'Isola, L. Stabile, A. Viola, Uncertainty budget of the SMPS–APS system in the measurement of PM1, PM2.5, and PM10, Aerosol. Sci. Technol. 43 (2009) 1130–1141, http://dx.doi.org/10.1080/02786820903204078.
[47] M. Zaatari, A. Novoselac, J. Siegel, The relationship between filter pressure drop, indoor air quality, and energy consumption in rooftop HVAC units, Build. Environ. 73 (2014) 151–161, http://dx.doi.org/10.1016/j.buildenv.2013.12.010.
[48] M. Geller, S. Biswas, C. Sioutas, Determination of particle effective density in urban environments with a differential mobility analyzer and aerosol particle mass analyzer, Aerosol. Sci. Technol. 40 (2006) 709–723, http://dx.doi.org/10.1080/02786820600803925.
[49] M. Hu, J. Peng, K. Sun, D. Yue, S. Guo, A. Wiedensohler, Z. Wu, Estimation of size-resolved ambient particle density based on the measurement of aerosol number, mass, and chemical size distributions in the winter in beijing, Environ. Sci. Technol. (2012), http://dx.doi.org/10.1021/es204073t 120830075118007.
[50] M. Pitz, O. Schmid, J. Heinrich, W. Birmili, J. Maguhn, R. Zimmermann, H.-E. Wichmann, A. Peters, J. Cyrys, Seasonal, Diurnal Variation, Of PM2.5 apparent particle density in urban air in augsburg, Germany, Environ. Sci. Technol. 42 (2008) 5087–5093, http://dx.doi.org/10.1021/es7028735.
[51] P. Azimi, D. Zhao, B. Stephens, Estimates of HVAC filtration efficiency for fine and ultrafine particles of outdoor origin, Atmos. Environ. 98 (2014) 337–346, http://dx.doi.org/10.1016/j.atmosenv.2014.09.007.
[52] W. Jiao, G. Hagler, R. Williams, R. Sharpe, R. Brown, D. Garver, R. Judge, M. Caudill, J. Rickard, M. Davis, L. Weinstock, S. Zimmer-Dauphinee, K. Buckley, Community Air Sensor Network (CAIRSENSE) project: evaluation of low-cost sensor performance in a suburban environment in the southeastern United States, Atmospheric Meas. Tech 9 (2016) 5281–5292, http://dx.doi.org/10.5194/amt-9-5281-2016.
[53] J.M. Delgado-Saborit, Use of real-time sensors to characterise human exposures to combustion related pollutants, J. Environ. Monit. 14 (2012) 1824, http://dx.doi.org/10.1039/c2em10996d.
[54] C. Lin, J. Gillespie, M.D. Schuder, W. Duberstein, I.J. Beverland, M.R. Heal, Evaluation and calibration of Aeroqual series 500 portable gas sensors for accurate measurement of ambient ozone and nitrogen dioxide, Atmos. Environ. 100 (2015) 111–116, http://dx.doi.org/10.1016/j.atmosenv.2014.11.002.
[55] L. Deville Cavellin, S. Weichenthal, R. Tack, M.S. Ragettli, A. Smargiassi, M. Hatzopoulou, Investigating the use of portable air pollution sensors to capture the spatial variability of traffic-related air pollution, Environ. Sci. Technol. 50 (2016) 313–320, http://dx.doi.org/10.1021/acs.est.5b04235.
[56] C.M. Torrey, K.A. Moon, D.A.L. Williams, T. Green, J.E. Cohen, A. Navas-Acien, P.N. Breysse, Waterpipe cafes in Baltimore, Maryland: carbon monoxide, particulate matter, and nicotine exposure, J. Expo. Sci. Environ. Epidemiol. 25 (2015) 405–410, http://dx.doi.org/10.1038/jes.2014.19.
[57] S. Zhou, L. Behrooz, M. Weitzman, G. Pan, R. Vilcassim, J.E. Mirowsky, P. Breysee, A. Rule, T. Gordon, Secondhand hookah smoke: an occupational hazard for hookah bar employees, Tobac. Contr. (2016), http://dx.doi.org/10.1136/tobaccocontrol-2015-052505.
[58] B. Less, N. Mullen, B. Singer, I. Walker, Indoor air quality in 24 California residences designed as high-performance homes, Sci. Technol. Built Environ 21 (2015) 14–24, http://dx.doi.org/10.1080/10789669.2014.961850.
[59] ASHRAE, ASHRAE Handbook of Fundamentals: Chapter 1: Psychrometrics, (2013).
[60] Weather Underground, PWS Data: West Loop KILCHICA403, Pers. Weather Stn. Netw, (2017) https://www.wunderground.com/personal-weather-station/dashboard?ID=KILCHICA403.
[61] P. Ellis, P. Torcellini, Simulating Tall Buildings Using EnergyPlus, 2005 Montreal, Canada http://www.ibpsa.org/proceedings/bs2005/bs05_0279_286.pdf.
[62] L. Leung, P. Weismantle, Sky-sourced Sustainability: How Super Tall Buildings Can Benefit from Height, Council on Tall Buildings and Urban Habitat, Dubai, 2008, http://www.ctbuh.org/LinkClick.aspx?fileticket=bYVa4k5GTS8%3D&tabid=1720&language=en-GB.
[63] Z. Tong, Y. Chen, A. Malkawi, Estimating natural ventilation potential for high-rise buildings considering boundary layer meteorology, Appl. Energy 193 (2017) 276–286, http://dx.doi.org/10.1016/j.apenergy.2017.02.041.
[64] US EPA, Download Detailed AQS Data, (2013) Technol. Transf. Netw. TTN Air Qual. Syst. AQS http://www.epa.gov/ttn/airs/airsaqs/detaildata/downloadaqsdata.htm (accessed January 13, 2014).
[65] J. Sailor David, A review of methods for estimating anthropogenic heat and moisture emissions in the urban environment, Int. J. Climatol. 31 (2011) 189–199, http://dx.doi.org/10.1002/joc.2106.